Citation for published version:
Topolov, VY & Bowen, CR 2015, 'High-performance 1-3-type lead-free piezo-composites with auxetic polyethylene matrices', Materials Letters, vol. 142, pp. 265-268. https://doi.org/10.1016/j.matlet.2014.12.018

DOI:
10.1016/j.matlet.2014.12.018

Publication date:
2015

Document Version
Early version, also known as pre-print

High-performance 1–3-type lead-free piezo-composites with auxetic polyethylene matrices

V.Yu. Topolov[a,*] and C.R. Bowen[b]

[a]Department of Physics, Southern Federal University, 5 Zorge Street, 344090 Rostov-on-Don, Russia

[b]Department of Mechanical Engineering, University of Bath, Bath BA2 7AY, UK

ABSTRACT High piezoelectric sensitivity and large hydrostatic parameters are discussed for two types of 1–3-type single crystal/auxetic polymer composites. The single crystal components selected are based on lead free $(K,Na)(Nb,Ta)O_3$ and $(Li,K,Na)(Nb,Ta)O_3$ solid solutions, and the auxetic polymers are characterised by Poisson's ratios $-0.83 \le \nu \le -0.29$. The composites examined exhibit advantageous properties over conventional lead-based piezo-active composites and ceramics such as high longitudinal piezoelectric coefficient $g_{33}^* \sim (10^2–10^3)$ mV·m/N, squared figure of merit $(Q_{33}^*)^2 \sim 10^{-11}$ Pa^{-1}, hydrostatic piezoelectric coefficient $g_h^* \sim (10^2–10^3)$ mV·m/N and squared figure of merit $(Q_h^*)^2 \sim (10^{-11}–10^{-10})$ Pa^{-1}. The composites also demonstrate an infinitely large anisotropy of piezoelectric coefficients d_{3j}^*.

Keywords: Composite materials; Elastic properties; Ferroelectrics; Polymers; Piezoelectric materials

*Corresponding author. Tel.:+7 8632975127; fax:+7 8632975120. E-mail:vutopolov@sfedu.ru

1. Introduction

Piezo-composites are an important group of modern smart materials with tailored and high-performance properties. As a rule, these composites are based on perovskite-type ferroelectrics – either poled ceramics (often of the PZT or $PbTiO_3$ type) or domain-engineered single crystals (SC) such as $(1–x)Pb(Mg_{1/3}Nb_{2/2})O_3–xPbTiO_3$ (PMN–xPT) and $(1–x)Pb(Zn_{1/3}Nb_{2/2})O_3–xPbTiO_3$ [1,2]. In the last decade environmental concerns have led to attempts to eliminate lead-based materials from consumer items, including piezoelectric transducers, sensors and actuators. The need for lead-free ferroelectrics gives rise to the challenge of finding an alternative [3], to conventional lead-based ferroelectric ceramics and single crystals, which exhibit high piezoelectric activity to enhance the effective electromechanical properties of piezo-composites [2]. Recent experimental studies of ferroelectric modified niobate solid solutions [4,5] suggest that these lead-free materials in the form of SCs can be used as the main component in modern composites, for instance, due to large piezoelectric d_{33} and g_{33} coefficients (see, e.g., Table 1). However no work on the piezoelectric performance of lead-free composites is yet to be published, and no trends in the use of lead-free ferroelectric SCs or ceramics have been discussed in the context of composite components, design and properties. The aim of this paper is to provide the first detailed demonstration of ability to achieve high-performance novel piezo-composites based on the SCs from Table 1. Such data will provide composite designers routes to design lead-free piezo-composite transducers with predictable and useful properties.

2. 1–3-type composites and their effective parameters

The composite considered is shown in Fig.1 and contains a system of ferroelectric SC rods in the form of rectangular parallelepipeds which are continuous in the OX_3 direction, having a square base and characterised by a square arrangement in the (X_1OX_2) plane. The rods are poled along the [001] direction of the perovskite unit cell, and the main crystallographic axes x, y and z of each SC rod obey the conditions x||[001], y||[010] and z||[001]. The polymer is a passive auxetic microporous polyethylene (PE-n, n= 1,2,... 9) with a negative Poisson's ratio whose elastic properties have been reported in [6], and are shown in Table 2. It is assumed that the relative dielectric permittivity of PE-n equals 2.3, as is the case for monolithic PE [7]. As a result of the microporous structure of the PE-n [6] matrix (Fig.1) the composite is described by a 1–3–γ connectivity, i.e., it belongs to the 1–3 type in terms of work [2].

The effective electromechanical properties of the composite in Fig.1 are determined using the matrix method [2]. For m=const the elastic compliances s_{ab}^{*E} (at electric field E=const), piezoelectric coefficients d_{ij}^{*} and dielectric permittivities $\varepsilon_{ff}^{*\sigma}$ (at mechanical stress σ=const) are evaluated. Based on these properties, the effective parameters $\Pi^*=\Pi^*(m)$ are analysed as follows: the piezoelectric coefficient g_{33}^{*} (from $d_{kl}^{*}=\varepsilon_{fk}^{*\sigma}\, g_{fl}^{*}$), squared figure of merit $(Q_{33}^{*})^2=d_{33}^{*}\, g_{33}^{*}=(d_{33}^{*})^2/\varepsilon_{33}^{*\sigma}$, thickness electromechanical coupling factor (ECF) $k_t^* = [(c_{33}^{*D} - c_{33}^{*E})/c_{33}^{*D}]^{1/2}$, and hydrostatic parameters such as $d_h^* = d_{33}^* + d_{32}^* + d_{31}^*$, $g_h^* = g_{33}^* + g_{32}^* + g_{31}^*$, squared figure of merit $(Q_h^*)^2 = d_h^* g_h^*$ and ECF $k_h^* = d_h^* (s_h^{*E} \varepsilon_{33}^{*\sigma})^{-1/2}$, where c_{33}^{*D} and c_{33}^{*E} are elastic moduli at electric displacement D=const and electric field E=const, respectively, and s_h^{*E} is the hydrostatic elastic compliance at E=const. The parameters g_{33}^* and $(Q_{33}^*)^2$ characterise the longitudinal sensitivity, and $(Q_{33}^*)^2$ is also linked to the sensor signal-to-noise ratio [2]. In hydrophone applications d_h^* and g_h^* characterise the piezoelectric activity and sensitivity, respectively. The parameter $(Q_h^*)^2$ is a hydrostatic analog of $(Q_{33}^*)^2$ and describes the effectiveness of the material as a hydrophone and actuator. The ECFs k_t^* and k_h^* describe the efficiency of the conversion of electric energy into mechanical energy and vice versa at the thickness oscillation mode (subscript 't') or under hydrostatic loading (subscript 'h').

Table 3 shows the largest maximum values of effective parameters of the lead free composites. It can be seen that PE-5 and PE-8 show the highest 'activity' in achieving the largest max$\Pi^*(m)$ values irrespective of the type of SC, and the next important polymer is PE-9. PE-5 is characterised by the largest elastic compliance s_{11} (Table 2) which strongly influences the piezoelectric response along the OX_3 direction. PE-8 and PE-9 have Poission's ratios $\nu < -0.5$, however the s_{11} of PE-8 is larger and promotes a stronger piezoelectric response along OX_3. It should be highlighted that the manufacture of composites with such small SC volume fractions (m<0.05), which are related to max g_{33}^*, max g_h^* and max$[(Q_h^*)^2]$, can be challenging. Fig.2 show the ranges wherein g_{33}^*, g_h^*, $(Q_{33}^*)^2$, and $(Q_h^*)^2$ vary at m=0.05 and 0.10. Changes in g_{33}^* are in a relatively narrow range and related to moderate changes in s_{11} of PE-n (Table 2). The changes in $(Q_{33}^*)^2$ are more distinct in comparison to g_{33}^*; this is a result of a rapid increase in d_{33}^* and a slow increase in $\varepsilon_{33}^{*\sigma}$ in the 1–3-type SC/polymer composite [2]. Changes in both g_h^* and $(Q_h^*)^2$ are predominantly the result of the elastic properties of PE-n with a negative Poisson ratio ν that promotes a validity of inequalities $g_h^* > g_{33}^*$ and $(Q_h^*)^2 > (Q_{33}^*)^2$ due to positive contributions from $d_{31}^*, d_{32}^*, g_{31}^*$, and g_{32}^* in wide ranges of volume-fraction. The larger values of g^*_{33}, g^*_h, $(Q^*_{33})^2$, and $(Q^*_h)^2$ in Fig.2,a,c in comparison to those in Fig.2,b,d stem from the fact that the piezoelectric coefficient d_{33} of KNN-TL is approximately 2.2 times larger than d_{33} of KNN-T (Table 2).

The use of auxetic polymers leads to a non-monotonic behaviour of the piezoelectric coefficient d^*_{31} and

$$d^*_{31}(m^*)=0. \quad (1)$$

While Eq.(1) holds, the piezoelectric anisotropy of the composite $d^*_{33}/|d^*_{31}|\to\infty$, and its hydrostatic parameters obey equalities $d^*_h=d^*_{33}$, $g^*_h=g^*_{33}$, $(Q^*_h)^2=(Q^*_{33})^2$, and $k^*_h=d^*_{33}(s^{*E}_h\,\varepsilon^{*\sigma}_{33})^{-1/2}$. However, our findings show that d^*_{33}, g^*_{33} and $(Q^*_{33})^2$ change in wide ranges, as seen in Fig.3,a,c, while k^*_h and k^*_t undergo minor changes (Fig.3,b,d) when replacing PE-*n* at *m*=*m** from Eq.(1). Due to the 1–3-type composite structure (Fig.1), the condition $k^*_t=k^*_{33}$ is valid with an accuracy to 3% at *m*=*m**. The correlation between the volume fraction *m** and Poisson ratio ν (Fig.3,e) highlights the key role of the elastic properties of the polymer matrix in achieving an infinitely large piezoelectric anisotropy for the composite.

The composites studied here show particular advantages over some piezo-active lead-containing composites and ceramics. For instance, for a 1–3 PMN–0.30PT SC /epoxy composite [1] max g^*_{33}= 440 mV·m/N (at a small volume fraction *m*=0.018) which is approximately 1.5 times smaller than g^*_{33} of the KNN-T-based composite (see Fig.2,c,d). The values of g^*_h shown in Fig.2 are approximately 5–16 times more than the max g^*_h of 1–3 PMN–*x*PT SC/araldite and PZN–*x*PT SC/araldite composites, and the $(Q^*_h)^2$ values (Fig.2) are 20–43 times more than values of max$[(Q^*_h)^2]$ of the aforementioned lead-based 1–3 composites [2]. The effective parameters shown in Fig.3 can also be compared to those of highly anisotropic ferroelectric ceramics. For example, a modified $PbTiO_3$ ceramic [8] is characterised by d_{33}= 51 pC/N and g_{33}= 32.6 mV·m/N at d_{33}/d_{31}=

–11.6, i.e., the d_{33} and g_{33} of this ceramic are smaller than d_{33}^* and g_{33}^* of the KNN-TL- and KNN-T-based composites (Fig.3) at $d_{33}^*/|d_{31}^*|\to\infty$.

3. Conclusions

The letter provides the first detailed examination of lead-free 1–3-type SC/auxetic PE-*n* composites which can be regarded as advanced materials with high piezoelectric sensitivity [g_{33}^*~(10^2–10^3) mV·m/N], large squared figures of merit [$(Q_{33}^*)^2$~10^{-11} Pa^{-1}] and change in the sign of the piezoelectric coefficient d_{31}^*. Eq.(1) holds due to the auxetic polymer matrix and opens up possibilities of achieving a very large piezoelectric anisotropy at d_{33}^*~10^2 pC/N and k_{33}^*≈0.7–0.8. The hydrostatic piezoelectric response is characterised by g_h^*~(10^2–10^3) mV·m/N, $(Q_h^*)^2$~(10^{-11}–10^{-10}) Pa^{-1} and k_h^*≈0.3–0.4 at the thickness ECF k_t^*≈0.7–0.8. A comparative study has been undertaken on the performance of the 1–3-type piezo-composites that contain auxetic polymers. The results indicate there is potential for the use of lead-free piezo-composites as active elements of piezoelectric sensors, transducers, hydrophones, acoustic, and energy-harvesting devices.

Acknowledgements. Prof.Dr. C.R.Bowen acknowledges funding from the European Research Council under the European Union's Seventh Framework Programme (FP/2007-2013) / ERC Grant Agreement no.320963 on Novel Energy Materials, Engineering Science and Integrated Systems (NEMESIS). The work has been performed using the equipment of the Centre of Collective Use "High Technologies" at the Southern Federal University within the framework of the project RFMEFI59414X0002, and Prof.Dr. V.Yu.Topolov acknowledges the financial support thereby.

References

[1] Wang F, He C, Tang Y. Single crystal $0.7Pb(Mg_{1/3}Nb_{2/3})O_3$–$0.3PbTiO_3$ epoxy 1–3 piezoelectric composites prepared by the lamination technique. Mater Chem Phys 2007;105:273–7.

[2] Topolov VYu, Bowen CR. Electromechanical properties in composites based on ferroelectrics. London: Springer; 2009.

[3] Priya S, Nahm S, editors. Lead-free piezoelectrics. New York, Dordrecht, Heidelberg, London: Springer;

2012.

[4] Zheng L, Huo X, Wang R, Wang J, Jiang W, Cao W. Large size lead-free (Na,K)(Nb,Ta)O_3 piezoelectric single crystal: growth and full tensor properties. CrystEngComm 2013;15:7718–22.

[5] Huo X, Zheng L, Zhang R, Wang R, Wang J, Sang S, Wang Y, Yang B, Cao W. A high quality lead-free (Li, Ta) modified (K, Na)NbO_3 single crystal and its complete set of elastic, dielectric and piezoelectric coefficients with macroscopic 4*mm* symmetry. CrystEngComm 2014;16:9828–33.

[6] Evans KE, Alderson KL. The static and dynamic moduli of auxetic microporous polyethylene. J Mater Sci Lett 1192;11:1721–4.

[7] Groznov IN. Dielectric permittivity. In: Physics encyclopaedia. Moscow: Sovetskaya Entsiklopediya; 1983, p. 178–9 (in Russian).

[8] Ikegami S, Ueda I, Nagata T. Electromechanical properties of $PbTiO_3$ ceramics containing La and Mn. J Acoust Soc Am 1971;50:1060–6.

Table 1. Room-temperature elastic compliances s_{ab}^{E} (in 10^{-12} Pa^{-1}), piezoelectric coefficients d_{ij} (in pC/N) and relative dielectric permittivities $\varepsilon_{fr}^{\sigma}/\varepsilon_0$ of ferroelectric SCs (4*mm* symmetry)

SC	s_{11}^E	s_{12}^E	s_{13}^E	s_{33}^E	s_{44}^E	s_{66}^E	d_{31}	d_{33}	d_{15}	$\varepsilon_{11}^{\sigma}/\varepsilon_0$	$\varepsilon_{33}^{\sigma}/\varepsilon_0$
$(K_{0.562}Na_{0.438})\cdot(Nb_{0.768}Ta_{0.232})O_3$ (KNN-T) [4]	11.9	–4.30	–5.60	15.5	12.0	10.7	–77.0	162	45.0	291	267
$[Li_x(K_{0.501}Na_{0.499})_{1-x}]\cdot(Nb_{0.660}Ta_{0.340})O_3$ (KNN-TL) [5]	17.2	–5.11	–10.7	27.0	15.4	13.9	–163	354	171	1100	790

Table 2. Room-temperature elastic compliances of auxetic PE-*n* [6]

n	1	2	3	4	5	6	7	8	9
s_{11}, 10^{-10} Pa^{-1}	1.97	2.36	2.02	2.10	2.72	2.59	1.88	2.36	2.30
s_{12}, 10^{-10} Pa^{-1}	0.571	0.755	0.646	0.735	1.14	1.17	0.921	1.37	1.91

Table 3. Largest maximum values of effective parameters of composites

	$\max g_{33}^*$, mV·m/N	$\max g_h^*$, mV·m/N	$\max[(Q_{33}^*)^2]$, 10^{-12} Pa^{-1}	$\max[(Q_h^*)^2]$, 10^{-12} Pa^{-1}	$\max d_h^*$, pC/N	$\max k_t^*$	$\max k_h^*$

KNN-T SC/auxetic PE-*n* composite							
Value	984	1730	59.5	160	142	0.830	0.477
At PE-*n*	PE-5	PE-8	PE-5	PE-8	PE-8	PE-5	PE-9
At *m*	0.022	0.022	0.055	0.042	0.132	0.595	0.095
KNN-TL SC/auxetic PE-*n* composite							
Value	706	1230	63.1	154	253	0.785	0.435
At PE-*n*	PE-5	PE-8	PE-5	PE-8	PE-5	PE-5	PE-8
At *m*	0.017	0.016	0.070	0.046	0.168	0.543	0.092

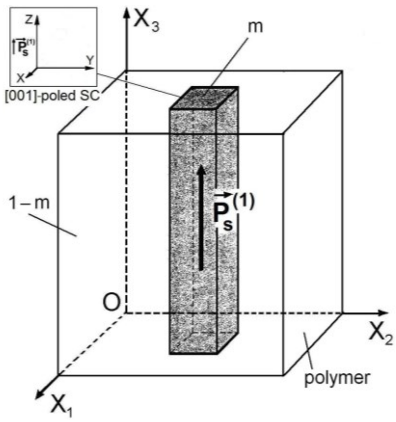

Fig. 1. Schematic of the SC/polymer composite. ($X_1X_2X_3$) is the rectangular co-ordinate system. *m* and 1–*m* are volume fractions of SC and polymer, respectively, x, y and z are main crystallographic axes of SC. The spontaneous polarisation vector of the SC rod $\boldsymbol{P}_s^{(1)}$ is shown via the arrow. SC rods with square bases are regularly distributed in the polymer matrix, and centres of symmetry of the bases form a simple square lattice in the (X_1OX_2) plane. Electrodes are to be applied parallel to the (X_1OX_2) plane.

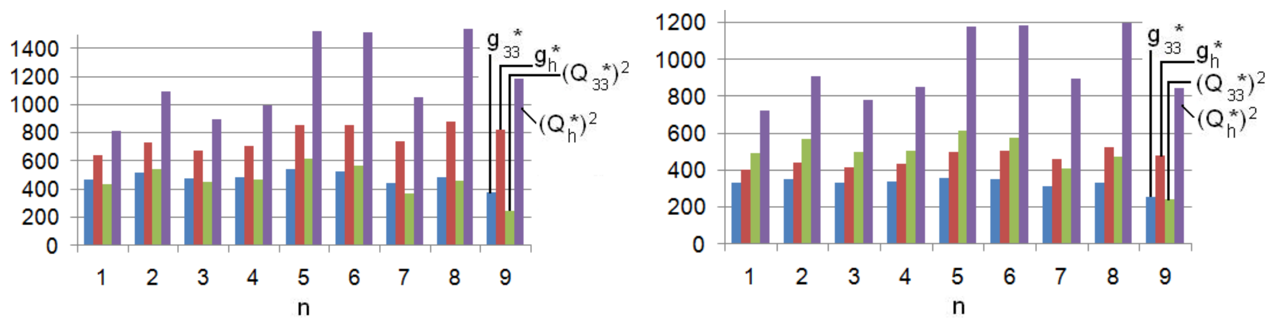

a b

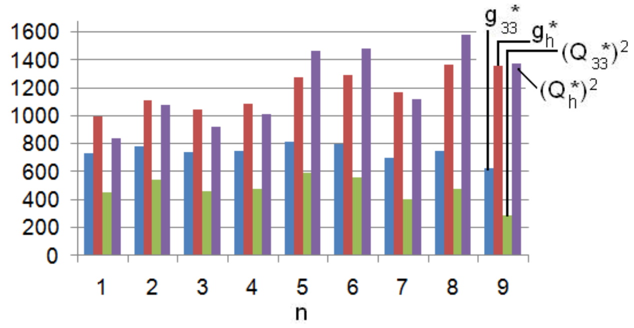

c

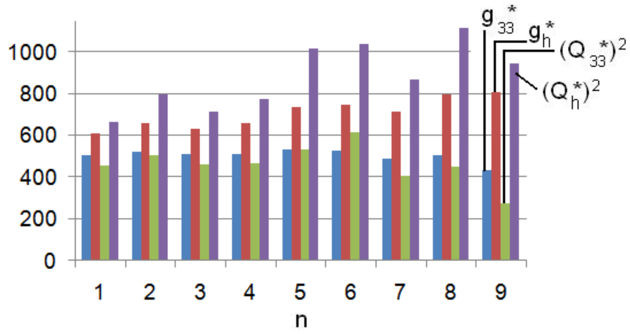

d

Fig. 2. Piezoelectric coefficients g_{33}^* and g_h^* (in mV·m/N) and squared figures of merit $(Q_{33}^*)^2$ and $(Q_h^*)^2$ (in 10^{-13} Pa^{-1}) of 1–3-type KNN-TL SC/auxetic PE-*n* (a,c) and KNN-T SC/auxetic PE-*n* (b,d) composites at *m*= 0.05 (a,b) and 0.10 (c,d).

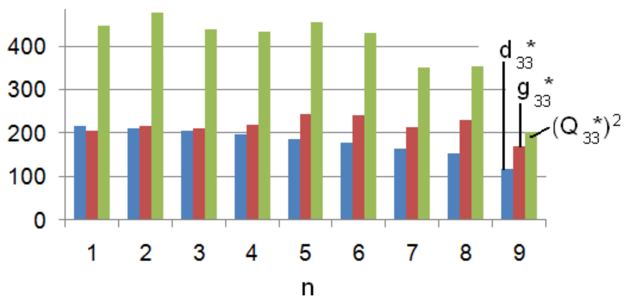

a

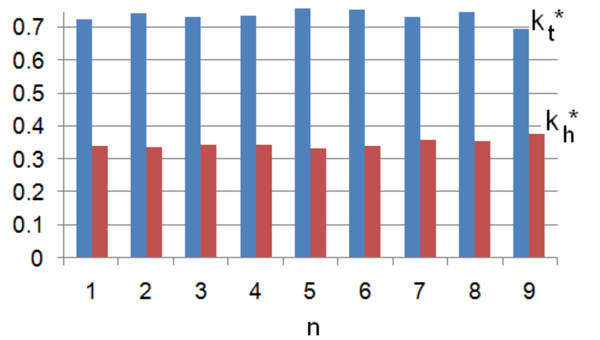

b

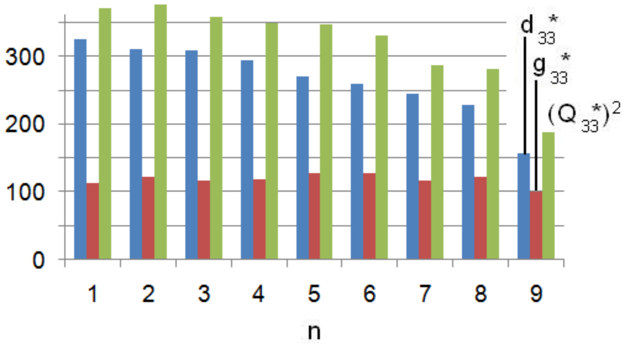

c

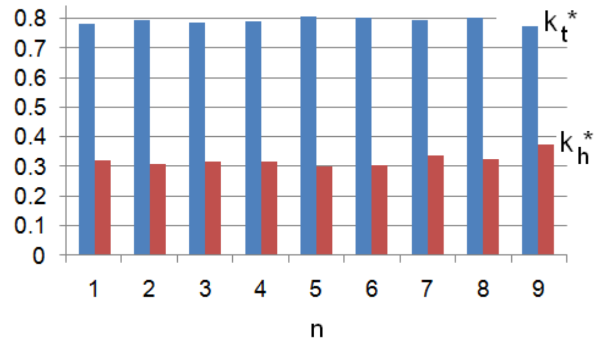

d

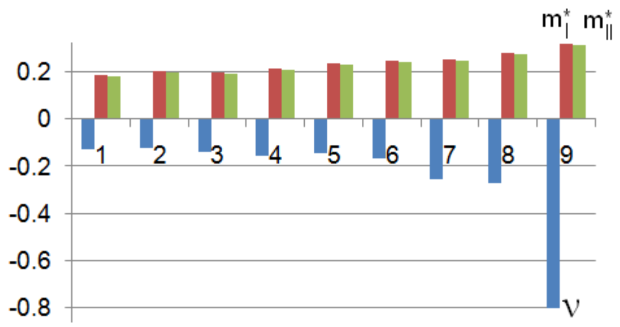

e

Fig. 3. Piezoelectric coefficients d_{33}^* (in pC/N), g_{33}^* (in mV·m/N), squared figure of merit $(Q_{33}^*)^2$ (in 10^{-13} Pa^{-1}) and ECFs k_t^* and k_h^* which are related to the 1–3-type KNN-T SC/auxetic PE-*n* composite at the volume fraction $m = m_I^*$ (a,b) and to the 1–3-type KNN-TL SC/auxetic PE-*n* composite at $m = m_{II}^*$ (c,d), volume fractions of SC m_I^* and m_{II}^*, which obey Eq.(1), and Poisson's ratios ν of PE-*n* (e).